Fast Muon Simulation in the JUNO Central Detector *

Lin Tao [1;1] Deng Zi-Yan [1] Li Wei-Dong [1] Cao Guo-Fu [1]
You Zheng-Yun [2] Li Xin-Ying [3]

[1] Institute of High Energy Physics, Chinese Academy of Sciences, Beijing 100049, China
[2] School of Physics, Sun Yat-sen University, Guangzhou 510275, China
[3] School of Physics, Nankai University, Tianjin 300071, China

arXiv:1602.00056v1 [physics.ins-det] 30 Jan 2016

Abstract: The Jiangmen Underground Neutrino Observatory (JUNO) is a multi-purpose neutrino experiment designed to measure the neutrino mass hierarchy using a central detector (CD), which contains 20 kton liquid scintillator (LS) surrounded by about 17,000 photomultiplier tubes (PMTs). Due to the large fiducial volume and huge number of PMTs, the simulation of a muon particle passing through the CD with the Geant4 toolkit becomes an extremely computation-intensive task. This paper presents a fast simulation implementation using a so-called voxel method: for scintillation photons generated in a certain LS voxel, the PMT's response is produced beforehand with Geant4 and then introduced into the simulation at runtime. This parameterisation method successfully speeds up the most CPU consuming process, the optical photon's propagation in the LS, by a factor of 50. In the paper, the comparison of physics performance between fast and full simulation is also given.

Key words: JUNO, Central Detector, Fast Simulation, Geant4

PACS: 29.40.Mc, 29.85.Fj

1 Introduction

The Jiangmen Underground Neutrino Observatory (JUNO)[1, 2] is a multiple purpose neutrino experiment to determine neutrino mass hierarchy and precisely measure oscillation parameters. It is being built in Jiangmen in Southern China and is about 53 km away from Yangjiang and Taishan nuclear power plants, respectively.

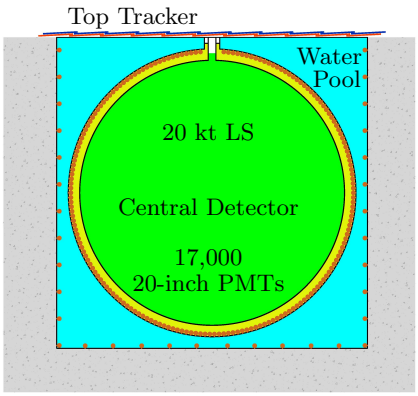

Fig. 1: (color online) Schematic view of the JUNO detector

The schematic view of the JUNO detector is shown in Fig. 1. The most inner part is called the central detector (CD). The CD is basically an acrylic sphere filled with 20 kt liquid scintillator (LS) and surrounded by about 17,000 20-inch photomultiplier tubes (PMTs). An energy resolution of $3\%/\sqrt{E(\mathrm{MeV})}$ is expected. Around the CD, there is a water pool to shield radioactivities. The PMTs in the water pool are used to detect the Cerenkov lights yielded by cosmic ray muons. On top of the water pool, there is a top tracker, made of plastic scintillators, to identify muon tracks.

To meet the requirement of high energy resolution for the CD, reliable and flexible Monte Carlo (MC) simulation software is a necessity, especially for optimizing detector parameters at the design stage. The simulation software has been developed based on the Geant4 [3] toolkit, which consists of a number of packages to manage event generators, geometry and materials, physics processes, tracking and user interfaces. Both optical parameters and physics processes have been tuned based on the experimental data obtained by the Daya Bay Neutrino Experiment[4]. The simulation software is highly integrated with the underlying software framework of SNiPER[5] so that it becomes an important component in the full data processing chain.

2 Data processing

The raw data recorded by the JUNO detector need to be processed offline in order to be converted to reconstructed data, which are suitable for physics analysis. In

* This work is supported by the Strategic Priority Research Program of the Chinese Academy of Sciences (Grant No. XDA10010900), National Natural Science Foundation of China (Grant No. 11405279, 11575224).

1) E-mail: lintao@ihep.ac.cn

the current phase, the raw data will be produced by the MC simulation and then are processed in the same way as the real data in the future. Following the scheme of SNiPER, various data processing steps shown in Fig. 2 are implemented as corresponding type of algorithms, software components undertaking certain amount of calculation task. Event data pass between different algorithms via a data buffer. The event data cached in the data buffer can be written to ROOT [6] files for persistent storage. The detector parameters stored in GDML [7] files can be accessed by algorithms through the detector description service in a uniform way.

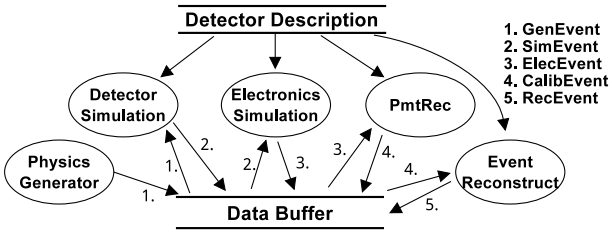

Fig. 2: Work flow for data processing

As shown in Fig. 2, the physics generator generates simulated physics events such as inverse β decay (IBD) events, cosmic ray muon events, radioactivity events and so on. The generated GenEvent objects, which are in the format of HepMC [8], mainly include kinematics information of the generated final-state particles. Then detector simulation loads GenEvent objects from the data buffer and starts tracking with Geant4. The information of simulated hits such as charge and time information are saved into SimEvent objects. After inputting SimEvent objects, electronics simulation performs digitization and generates ElecEvent objects containing information of waveforms with predefined sampling rate. Then the PmtRec algorithm processes the waveforms and converts them into CalibEvent objects using calibration constants. Finally, the event reconstruction algorithm reads in CalibEvent objects, performs event reconstructing and stores the produced RecEvent objects in the data buffer.

3 Challenge of muon simulation

The muon induced background is one of the main backgrounds in the JUNO experiment. The mean energy of muons that penetrate the overburden is about 215 GeV and they reach the JUNO detector at the rate of about 3 Hz [2].

When a muon travels through the CD, energy is deposited in the LS and both scintillation and Cerenkov photons are emitted: the formers are emitted isotropically, while the latters are produced with a fixed angle with respect to the muon track. The ratio Cerenkov over scintillation photons is only 5%. The yield for scintillation photons is given by the Birks' Law [9]. The number of scintillation photons, dS, as a function of the visible energy dE_{vis} is given by

$$dS = A \cdot dE_{vis} = A\frac{dE}{1+C_1\delta+C_2\delta^2}\ ,\ \delta = \frac{dE}{\rho dx}[\mathrm{MeVg^{-1}cm^2}]\ , \tag{1}$$

where dE is the energy loss, A is the light yield and C_1 and C_2 are Birks constants.

After an optical photon is emitted in the LS, it will travel in the LS and there is a certain possibility for it to reach a PMT after passing through the acrylic sphere and buffering water. During the photon's propagation, it might be absorbed or scattered. At the liquid scintillator and acrylic sphere boundary, it may be refracted, or reflected, or even a total internal reflection may occur. If it reaches the photo-cathode of a PMT, a photoelectron may be generated. The timing information of the photoelectron can be described by Eq. 2, where T_{start} is the initial time, ΔT_{gen} is the generation time of the scintillation photon, ΔT_{hit} is called hit time, which includes the optical photon's propagation time and the photoelectron's generation time.

$$T = T_{start} + \Delta T_{gen} + \Delta T_{hit}. \tag{2}$$

The MC simulation of muon particles is important for physics studies, but the full simulation with Geant4 is extremely CPU consuming. To simulate a muon with typical energy passing through the central detector, at least 50 minutes are required using a modern CPU core. So the generation of cosmic ray muons with full simulation becomes a big challenge. The most time consuming part is the propagation of optical photons due to the huge number of photons (at the level of 10^7).

4 Fast muon simulation

The scintillation photons make up the majority of optical photons generated by the muons passing through the CD. To speed up propagation process of scintillation photons, a fast simulation employing a so-called voxel method has been implemented. Instead of the full simulation, it models the response of the PMTs by sampling the response distributions prepared in advance with the Geant4 simulation.

4.1 Voxel method

In the voxel method, the volume of the whole liquid scintillator sphere is treated as a regular grid and a voxel represents the volume element in the grid. By dividing the sphere into voxels, a muon particle encounters a serial of voxels along its path when it enters the CD. In Fig. 3, the scintillation photons generated in the shaded voxel (fired voxel) reach the PMT and generate

detector response. The location relationship between the fired voxel and the PMT can uniquely be determined by a pair of variables (R, θ), where R is the radius of the voxel and θ is the spatial angle between the voxel and the PMT. If there is a certain amount visible energy of E_{vis} in a voxel, the response of the PMTs with the same (R, θ) pair value follows the same distributions. It is obvious that the response distributions can be easily obtained by running the full simulation. So the core of the voxel method is to build the connection between the E_{vis} in a voxel and the response of the PMTs.

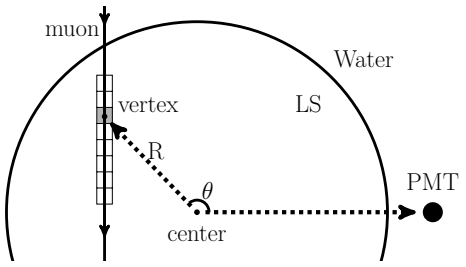

Fig. 3: Illustration of mapping the visible energy within a voxel to the response of the PMTs

At the stage of preparing response distributions, photons are produced uniformly in all LS voxels with the full simulation. Since photons with different wavelength behave differently in the detector, the emission spectrum of the LS is used to calculate the wavelength of the photons. For each voxel, the total number of generated photons is equivalent to the light yield of 1 MeV visible energy, which makes it possible for response distributions to contain sufficient information for the fast simulation to simulate a physics event. Photons received by each PMT and the associated timing information are the most important data to reflect optical photon's transportation process in the LS. So the number of photoelectrons (nPE) and hit time can be regarded as the major parameters of PMT response.

For simplicity, an R-θ parameter space is used to represent the set of possible combinations of (R, θ) values, in which R ranges from 0 to the inside radius of the acrylic sphere and θ is between 0 to π. Both R and θ are divided into a serial of intervals, respectively. Each 2-dimensional bin in parameter space is associated with a number of voxels and PMTs. For a specific bin, two histograms, one is for nPE distribution and the other for hit time distribution, are generated by the full simulation. After traversing all the bins in the parameter space, a complete set of response distributions are obtained. Fig. 4 shows a profile of mean hit time for scintillation photons within a bin in the R-θ parameter space, in which the x-axis represents R^3, the y-axis represents θ and the z-axis indicates the mean hit time. This figure shows that vertex at the edge of detector is influenced by the total internal reflection, so that the mean hit time is larger than the normal hit time.

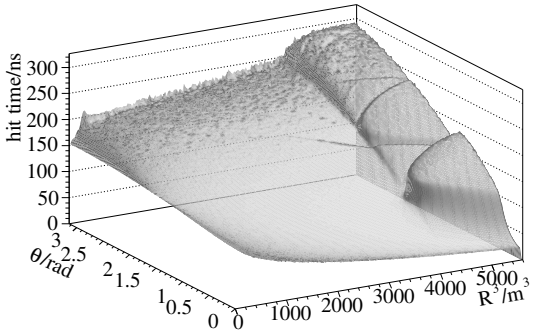

Fig. 4: Profile of mean hit time for scintillation photons within a bin in the R-θ parameter space.

At the stage of using the prepared response distributions to do the fast muon simulation, the procedure is as follows: for every step of muon tracking in LS, the visible energy, E_{vis}, is calculated according to the Birks' Law, which is the same as that in scintillation process. If the E_{vis} value is none-zero, the voxel that the tracking step encounters is identified by the step's position and the two associated nPE and hit time histograms are loaded. Then E_{vis} is broken into an integer part (floor of E_{vis}, $\lfloor E_{vis} \rfloor$) and a fractional part. Both are used to calculate nPE, as Eq. 3 shows, where N_{int} is the integer part and N_{frac} is the fractional part. For the integer part,the nPE histogram is sampled $\lfloor E_{vis} \rfloor$ times, as shown in Eq. 4. For the fractional part, the nPE histogram is sampled only once to get $N_{int}^{\lfloor E_{vis} \rfloor}$. N_{frac} follows the binomial distribution $N_{frac} \sim \mathrm{B}(N_{int}^{\lfloor E_{vis} \rfloor}, p)$, where the fractional part is used to calculate the probability for the PMT to be hit or not.

$$N = N_{int} + N_{frac} \tag{3}$$

$$N_{int} = \sum_{j=0}^{j<\lfloor E_{vis} \rfloor} N_{int}^{j} \tag{4}$$

If the PMT's nPE is greater than zero, its hit time is obtained by sampling the associated hit time histogram.

4.2 Performance measurements

The data sample used in the physics performance studies are single γs with the energy of 1 MeV, which are generated along vertical z axis with a step of 0.1 m in the LS. To guarantee sufficient statistics, 10,000 events are generated at each position.

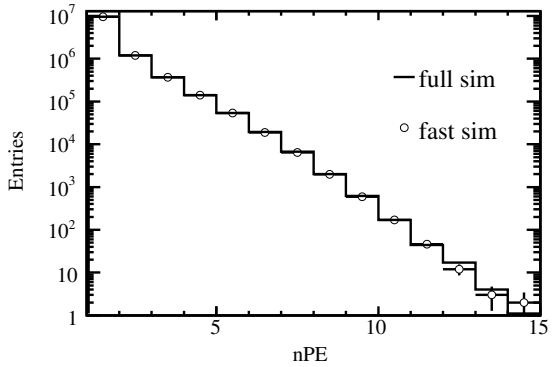

(a) nPE of PMT

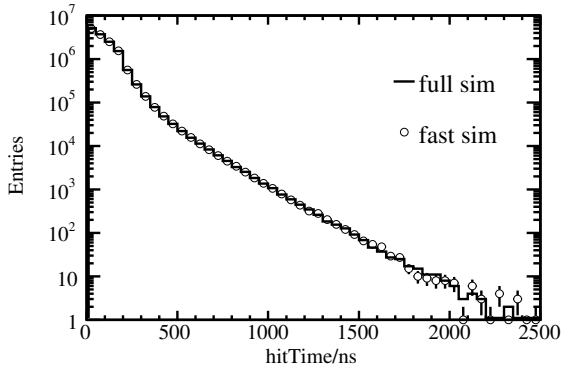

(b) Hit time of PMT

Fig. 5: Comparisons of nPE and hit time between fast and full simulation using γs generated at z=16 m.

As shown in Fig. 5, the distributions of nPE and hit time are compared respectively between the fast and full simulation using γs generated at z=16 m. It is obvious that the agreement is good for both nPE and hit time at the PMT level. The optical photons received by a PMT should have two components: photons directly from the interaction position and reflected photons. The closer to the acrylic sphere the γs are generated, the more optical photons are expected to be bounced back at the barrier due to the reflection effect. For γs generated at z=17.3 m, Fig. 6 shows the hit time distribution of some selected PMTs whose θ varies from 175° to 176°. According to MC truth information of the full simulation, the first peak is caused by the direct photons, however, the second one is mainly contributed by the reflected photons. So the fast simulation can reflect effectively the transportation of optical photons in the LS.

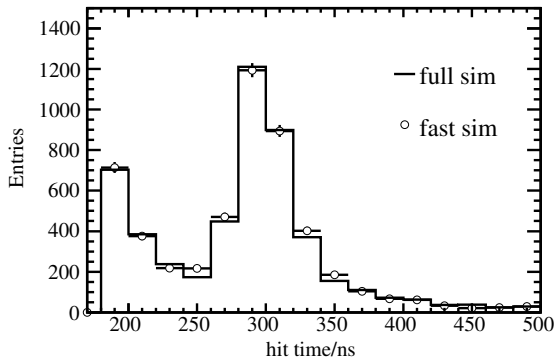

Fig. 6: Hit time of the PMTs in the region of 175° to 176° with γs generated at z=17.3 m.

Fig. 7 shows the average total number of photoelectrons per event (totalPE) as a function of γ's generation position z. The difference between fast and full simulation is less than 0.4%, which again demonstrates a good consistency between them. The totalPE increases with the γ's generation position getting closer to to the acrylic sphere. After reaching the turning point, the totalPE drops down mainly because of the total internal reflection and energy leak. So the fast simulation can model the change of totalPE with the vertex in a precise way.

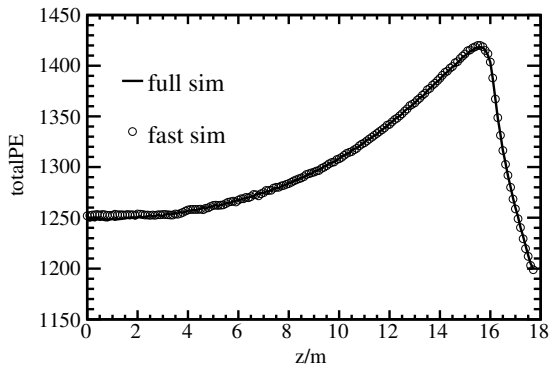

Fig. 7: Average totalPE as a function of γ's generation position z.

When a muon particle passes through the CD, the number of scintillation photons it generates is proportional to its visible energy in the liquid scintillator. So the more energy the muon particle deposits, the more CPU time is required to simulate the generation and transportation process of scintillation photons. To make a thorough timing measurement, a broad band of energy points covering 10 GeV, 100 GeV, 215 GeV, 500 GeV and 1 TeV is chosen for muon particle's generation. Ahead of timing measurements, a full simulation job is run and during job execution information at each MC simulation step are collected and stored in a data file. The prepared

data file will be used by the subsequent fast simulation so that it can be compared with the full simulation at event level. The measurement of system performance is done on a blade server with the CPU Intel® Xeon® E5-2680 v3 @ 2.50GHz. In order to eliminate interferences, the CPU is exclusively used by the timing measurement job and other irrelevant applications such as system monitoring are all suspended.

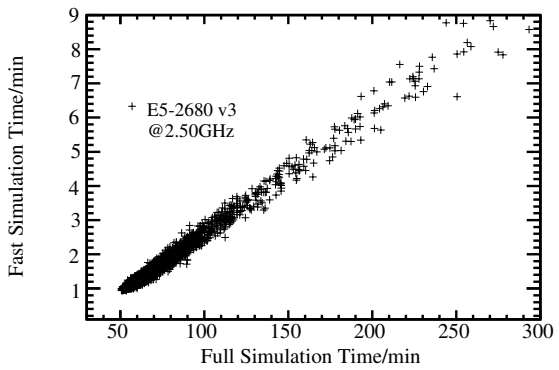

Fig. 8: The fast simulation time versus the full simulation time for muon particles with their momenta varying between 10 GeV and 1 TeV.

Fig. 8 is a scatter plot of execution time elapsed on generation and transportation of scintillation photons generated by muons passing through the central detector. Each cross represents the fast simulation time versus the full simulation time for a muon particle. The result shows that the elapsed simulation time scales linearly with the muon particle's visible energy and the fast simulation achieves a speedup ratio of about 50 over the full simulation.

4.3 Discussions

The JUNO CD simulation with Geant4 is largely dominated by optical photons' transportation in the liquid scintillator. Although the voxel method has been developed to speed up the muon simulation in the central detector, it can also be extended to simulate other types of events such as IBD because the parameterization approach is related to neither event types nor event energy.

The symmetry of detector geometry greatly reduces the number of sampling histograms used by the voxel method. But there are many factors that might break this kind of symmetry. For example supporting sticks around the acrylic sphere will block detection of optical photons. The voxel method can handle this problem by increasing the number of sampling histograms.

It is easy to use parallel computing technique such as CUDA [10] to further accelerate execution of the voxel method. Unlike the full simulation application running on GPU such as Chroma [11], the parallel implementation of voxel method can only execute histogram sampling with GPUs, which avoids the complexity of geometry translation.

5 Conclusions

The fast muon simulation using the voxel method has been implemented in the JUNO's offline software framework. The applied method is to generate the response of the PMTs beforehand, for photons produced in different voxels in the CD with Geant4 and then to introduce the response into the fast simulation by sampling the response histograms at runtime.

The timing measurement shows that the fast simulation has obtained a speedup ratio of 50 in CPU execution time compared to the full simulation with Geant4. The physics performance has also been examined and validation results show that the agreement between the fast and full simulation is good and no significant discrepancies have been found.

References

1 Z. Djurcic et al (JUNO Collaboration), arXiv:1508.07166
2 F.P. An et al (JUNO Collaboration), arXiv:1507.05613, accepted for publication in J. Phys. G.
3 S. Agostinelli et al (GEANT4 Collaboration), Nucl. Instrum. Meth. A, **506**: 250-303 (2003)
4 F. P. An et al (Daya Bay Collaboration), Phys. Rev. Lett.,**108**: 171803 (2012)
5 J. H. Zou et al, J. Phys. Conf. Ser., **664**(7): 072053 (2015)
6 R. Brun and F. Rademakers, Nucl. Instrum. Meth. A, **389**: 81-86 (1997)
7 R. Chytracek, J. McCormick, W. Pokorski and G. Santin, IEEE Trans. Nucl. Sci., **53**: 2892 (2006)
8 M. Dobbs and J. B. Hansen, Comput. Phys. Commun., **134**: 41-46 (2001)
9 J. B. Birks, Proc. Phys. Soc. A, **64**: 874 (1951)
10 https://docs.nvidia.com/cuda/cuda-c-programming-guide/, retrieved 10th March 2015
11 http://chroma.bitbucket.org/_downloads/chroma.pdf, retrieved 12th December 2015